International Journal of Pharmaceutics 400 (2010) 49–58

Contents lists available at ScienceDirect

International Journal of Pharmaceutics

journal homepage: www.elsevier.com/locate/ijpharm

Risperidone solid dispersion for orally disintegrating tablet: Its formulation design and non-destructive methods of evaluation☆

Ziyaur Rahman, Ahmed S. Zidan, Mansoor A. Khan*

Division of Product Quality and Research, Center of Drug Evaluation and Research, Food and Drug Administration, MD, USA

ARTICLE INFO

Article history:
Received 23 June 2010
Received in revised form 18 August 2010
Accepted 22 August 2010
Available online 27 August 2010

Keywords:
Risperidone
Methyl-β-cyclodextrin
Solid dispersion
Orally disintegrating tablet

ABSTRACT

The focus of present investigation was to assess the utility of non-destructive techniques in the evaluation of risperidone solid dispersions (SD) with methyl-β-cyclodextrin (MBCD) and subsequent incorporation of the SD into orally disintegrating tablets (ODT) for a faster release of risperidone. The SD was prepared by a solvent evaporation method and evaluated by scanning electron microscopy (SEM), Fourier transform infrared (FTIR), near infrared spectroscopy (NIR), NIR-chemical imaging (NIR-CI), powder X-ray diffraction (PXRD) and differential scanning calorimetry (DSC). DSC and XRD analysis indicated that crystallinity of SD has reduced significantly. FTIR showed no interaction between risperidone and MBCD. Partial least square (PLS) was applied to the NIR data for the construction of chemometric models to determine both components of the SD. Good correlations were obtained for calibration and prediction as indicated by correlation coefficients >0.9965. The model was more accurate and less biased in predicting the MBCD than risperidone as indicated by its lower mean accuracy and mean bias values. SD-3 (risperidone:MBCD, 1:3) was incorporated into ODT tablets containing diluent (D-mannitol, FlowLac® 100 or galenIQ™-721) and superdisintegrant (Kollidon® CL-SF, Ac-Di-Sol or sodium starch glycolate). Disintegration time, T_{50} and T_{90} were decreased in the formulations containing mannitol and Kollidon® CL-SF, but increased with galenIQ™-721 and sodium starch glycolate, respectively. NIR-CI images confirmed the homogeneity of SD and ODT formulations.

Published by Elsevier B.V.

1. Introduction

Many patients, particularly children and the elderly population find it inconvenient to ingest conventional solid dosage forms such as tablets and capsules due to an impaired ability to swallow. This leads to patient non-compliance and potentially prolonged duration of treatment. This issue can be addressed through the development of orally disintegrating dosage forms that disperse or dissolve in the saliva and are swallowed without water. Besides improving the acceptability and compliance of patients, ODTs have been investigated for their potential to increase the bioavailability through the enhancement of the dissolution rate (Ahmed and Aboul-Einien, 2007; Corveleyn and Remon, 1998). Additionally, pharmaceutical companies have another reason for the development of ODTs. At the end of the patent term of a drug, development of a new dosage form provides a life cycle extension of the product (Biradar et al., 2006).

Risperidone is a BCS class II compound with low solubility and highly permeability characterstics (Amidon et al., 1995; Mathot et al., 2006). The dissolution rate can be improved by the use of surfactants (Liu et al., 2006), complexation with cyclodextrins (Wang et al., 2009) and solid dispersions with water soluble agents such as poloxamer (Kanagale et al., 2008), polyethylene glycol (Rahman et al., 2010a) and polyvinylpyrollidone (Rahamathulla et al., 2008). Solid dispersions with water insoluble agents such as Eudragit® (Khan et al., 2000) and hydroxypropylmethyl cellulose phthalate (Chen et al., 2006) cause retardation of drug release.

Cyclodextrins (CD) are cyclic oligosaccharide with six to eight dextrose molecules joined through one to four carbons of dextrose (Brewster and Loftsson, 2007). Cyclodextrins have the property of forming inclusion complex with a number of hydrophilic and hydrophobic molecules. This phenomenon was shown by researchers as one of the techniques of alleviating the issue of solubility of water insoluble drug (Babu et al., 2008; Klein et al., 2009; Wang et al., 2009). This is further improved by synthesizing highly water soluble derivatives of cyclodextrin such as hydroxypropyl β-CD, sulphobutyl ether β-CD, randomly methylated β-CD, dimethyl-β-CD and maltosyl β-CD. There are a number of FDA approved drug products of water insoluble drugs which uti-

☆ The views and opinions expressed in this paper are only those of the authors, and do not necessarily reflect the views or policies of the FDA.

* Corresponding author at: FDA/CDER/DPQR, White Oak, LS Building 64, Room 1070, 10903 New Hampshire Ave, Silver Spring, MD 20993-002, USA.
Tel.: +1 301 796 0016; fax: +1 301 796 9816.
E-mail address: Mansoor.Khan@fda.hhs.gov (M.A. Khan).

0378-5173/$ – see front matter. Published by Elsevier B.V.
doi:10.1016/j.ijpharm.2010.08.025

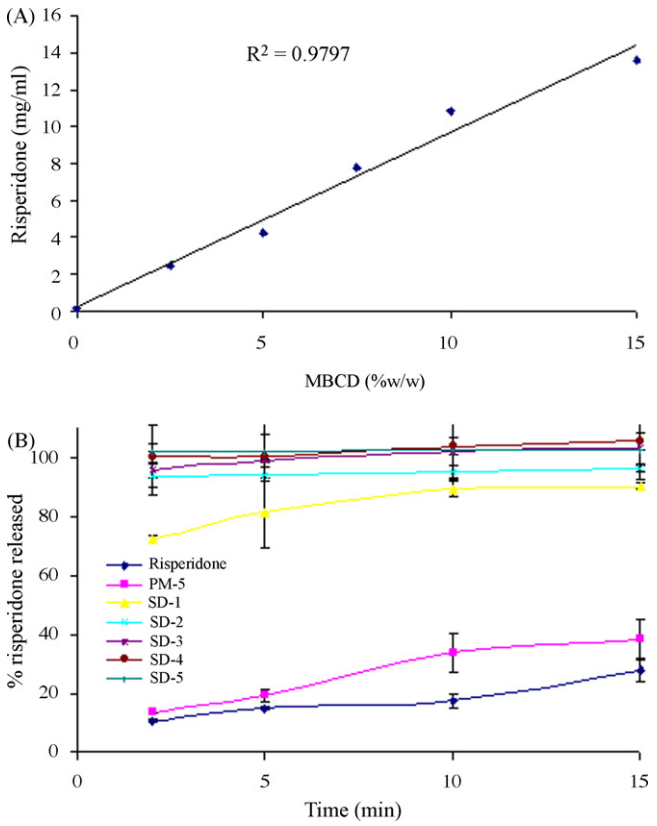

Fig. 1. (A) Phase solubility of risperidone in aqueous MBCD solution at 25 °C and (B) in vitro release profile of risperidone from SD formulations in USP phosphate buffer pH 6.0 at 37 °C.

lize cyclodextrin technology in the United States (Brewster and Loftsson, 2007). In addition to improving the solubility and taste masking of drugs (Patel and Vavia1, 2008), it also improves their physical and chemical stability (Cirri et al., 2009), absorption (Babu et al., 2008; Tewes et al., 2008) and bioavailability (Mannila et al., 2007; Ghorab et al., 2004).

Near infrared is a non-destructive technique for qualitative and quantitative analysis. It is widely used in medicinal diagnostics, food, agrochemistry, petrochemical and the pharmaceutical industry. It is a commonly used PAT tool for real time monitoring and control of pharmaceutical processes such as fluid bed processing (Alcala et al., 2009), mixing and blend uniformity (Sekulic et al., 1996; Sulub et al., 2009), drying (Dhopeshwarker et al., 2005) and high shear granulation (Rantanen et al., 2005). There is plethora of literature reporting the use of NIR as a non-destructive method for the estimation of components of physical blends and conventional formulations such as tablets (Li et al., 2009) and capsules (Ryan et al., 1991). Currently, there is a dearth of work showing the utility of NIR to estimate the components of complex dosage forms such as solid dispersions, microparticles, and liposomes. Previously, the authors reported the use of NIR to estimate the components of polylactic glycolic acid based nanoparticles, and polyethylene glycol and cyclosporine A solid dispersion dosage forms (Zidan et al., 2010; Rahman et al., 2010a).

In the present investigation, orally disintegrating tablets of risperidone were proposed based on solid dispersion and cyclodextrin technology. Secondly to estimate the individual components of the solid dispersion formulations by non-destructive methods, such as near infrared (NIR) and NIR-chemical imaging through the application of principal component (PCA) and partial least square (PLS) statistical methods.

2. Materials and methods

2.1. Materials

Risperidone was obtained from Erregierre S.p.A. (San Paolo D'Argon, BG). The following materials were obtained and used as-received, galenIQ™-721 (Palatinit GmbH, Mannheim, Germany), FlowLac® 100 (Molkerei Meggle Wasserburg GmbH and Co. KG, Wassergurg, Germany), Kollidon® CL-SF (BASF Chemicals Co., Florham, NJ, USA), magnesium stearate (Sigma-Aldrich, St. Louis, MO, USA), Ac-Di-Sol, Avicel PH 102 (FMC Biopolymer, Newark, DE, USA), methyl-β-cyclodextrin (MBCD, KLEPTOSE® CRYSMEB exp) and sodium starch glycolate Type-A (Roquette America Inc. Keokuk, IA, USA). D-mannitol, methanol and acetone were purchased from Fisher Scientific Co. (Norcross, GA, USA). All other reagents and solvents used were of analytical grade.

2.2. Methods

2.2.1. Phase solubility studies

Phase solubility was performed by adding excess amounts of risperidone to a solution of MBCD (0–15%, w/w) in water. The mixture of MBCD solution and risperidone was vortexed for 15 s and stirred using a horizontal shaker at 100 rpm at 25 °C for 48 h. The samples were filtered through a 0.22 μm Millipore nylon filter. The solubilized risperidone in the MBCD solution was determined by the HPLC method and studies were performed in triplicate.

2.2.2. Preparation of solid dispersion

The SD was prepared by solvent evaporation method (Rahman et al., 2010a). Ten SD formulations were prepared with varying ratios of drug to MBCD from 1:1 to 1:10 (SD-1 to SD-10). The batch size of each formulation was 2 g. In short, the drug and MBCD were dissolved in 20 ml of methanol and evaporated at room temperature for 24 h leaving solid residue. The material was further dried with a vacuum dryer at 30 °C for 48 h. The solid mass was milled and passed through 70 (ASTM) mesh sieve and refrigerated at 2–4 °C until further analysis. Three physical mixtures (PM-1, PM-3 and PM-5) were also prepared by trituration of risperidone and MBCD in a mortar and pestle and their compositions were equivalent to SD-1, SD-3 and SD-5 formulations, respectively.

2.2.3. In vitro release study

The in vitro release from SD and PM-5 was performed by a horizontal shaker method (Rahman et al., 2006) using USP phosphate buffer pH 6.0 as the dissolution medium at 100 rpm and 37 °C. The SD formulation equivalent to 4 mg of risperidone was transferred into a beaker containing 100 ml of phosphate buffer and a 1 ml aliquot was withdrawn at 2, 5, 10 and 15 min and analyzed for the amount of risperidone released into the medium by the HPLC method described below.

2.2.4. HPLC analysis

Risperidone was quantified from the SD formulation and ODT by modification of a reported HPLC method (Suthar et al., 2009). The HPLC equipment used was an HP 1050 (Agilent technologies, CA, USA) fitted with quaternary pumps, autosampler, and UV detector set to a wavelength of 280 nm and a column compartment thermostatted at 26 °C. The HPLC stationary phase was composed of a reverse phase Luna C18 (2) 4.6 mm × 250 mm (5 μm packing) column and a C18, 4.6 mm × 12.5 mm (5 μm packing) Luna C18 (2) guard column (Phenomenex Torrance, CA, USA). The mobile phase consisted of phosphate buffer (20 mM) pH 7.0: acetonitrile: methanol (40:45:15) and was pumped isocratically at a flow rate of 1 ml/min.

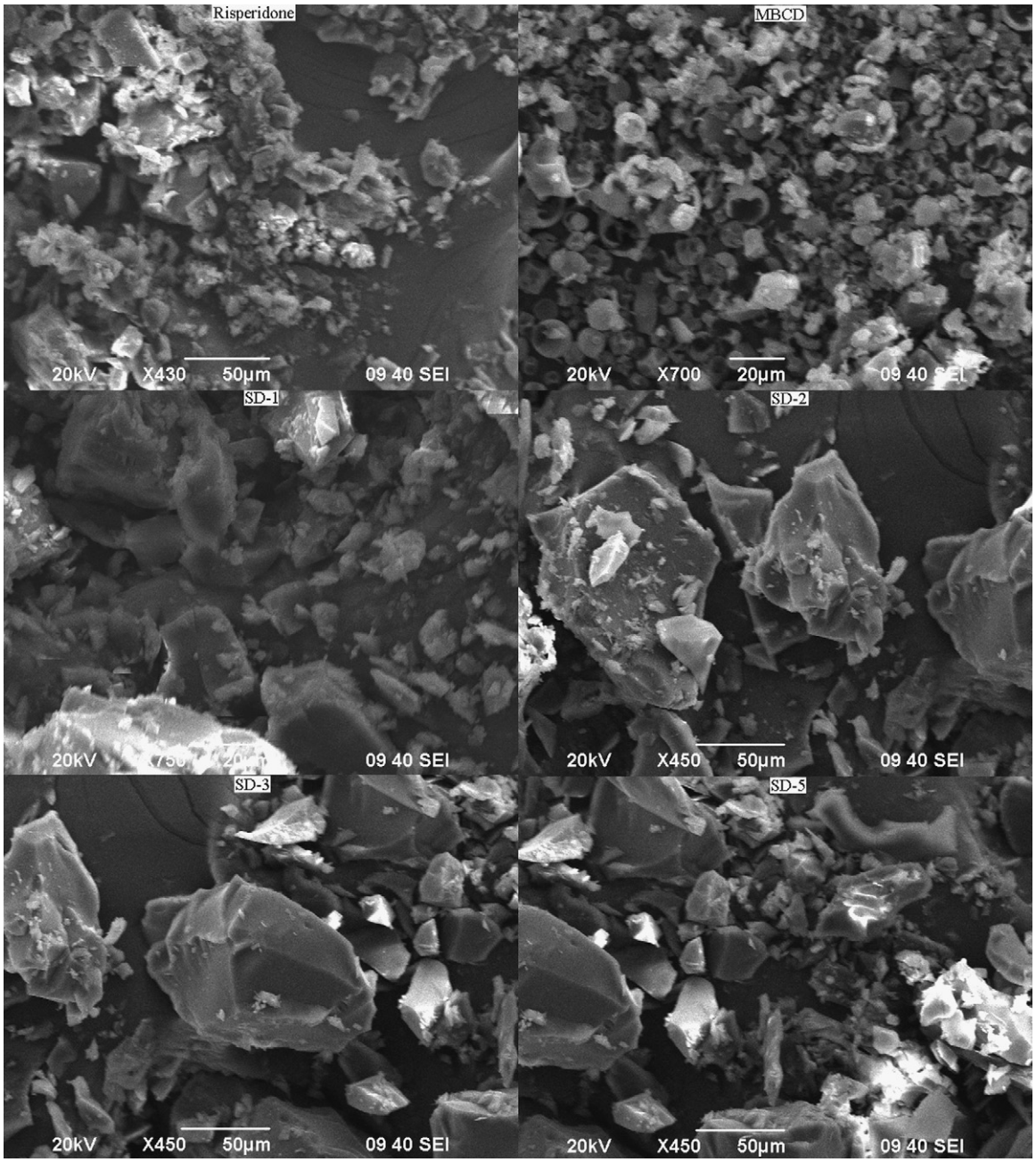

Fig. 2. SEM photomicrographs of risperidone, MBCD and SD formulations.

The HPLC method was validated as per ICH guidance (ICH, 2005).

2.2.5. Scanning electron microscopy

Shape and surface morphology characterization of risperidone, MBCD and SD formulations was performed by scanning electron microscopy (SEM, JSM-6390 LV, JEOL, Tokyo, Japan) measured at the working distance of 15 mm and an accelerated voltage of 20 kV. Samples were gold coated with a sputter coater (Desk V, Denton Vacuum, NJ, USA) before SEM observation under high vacuum 70 mTorr and high voltage of 30 mV.

2.2.6. Differential scanning calorimetry

Differential scanning calorimetry thermograms (DSC) of risperidone, MBCD, their physical mixtures and SD formulations was performed by a SDT 2960 Simultaneous DSC/TGA (TA Instruments Co., New Castle, DE, USA). Nitrogen gas flowed at 20 psi to create the inert atmosphere to prevent any oxidation reaction in the sample holder. The equipment was calibrated for baseline and temperature with indium metal. The sample was hermetically sealed in an aluminum pan and run from 10 to 200 °C at a scanning rate of 10 °C/min.

2.2.7. Fourier transform infrared spectroscopy

FTIR (Fourier transform infrared spectroscopy) spectra of pure components, their physical mixture and SD formulations were performed by attenuated total reflectance FTIR instrument (Thermo Nicolet Nexus 670 FTIR, GMI Inc., Ramsey, Minnesota, USA). OMNIC ESP software (version 5.1) was used to capture and analyze the spectra.

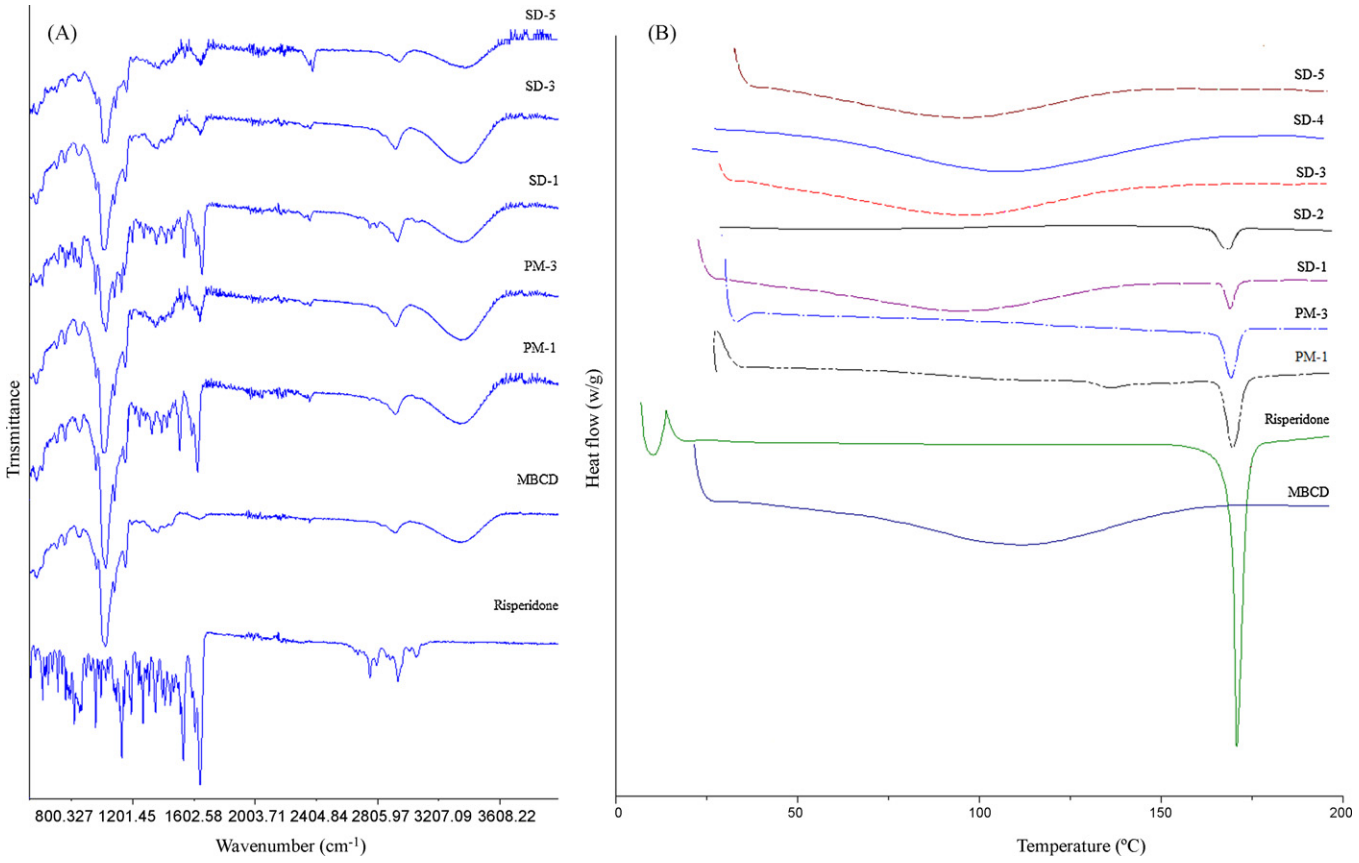

Fig. 3. (A) Fourier transform infrared spectra and (B) DSC thermogram of risperidone, MBCD, their physical mixtures and SD formulations.

2.2.8. Powder X-ray diffraction

Powder X-ray diffraction (PXRD) patterns of risperidone, MBCD, their physical mixture and SD formulations was collected using X-ray diffractometer (MD-10 mini diffractometer, MTI Corporation, Richmond, CA, USA) using Cu K2α rays (λ = 1.54056 Å) with a voltage of 25 kV and a current of 30 mA, in a flat plate $\theta/2\theta$ geometry, over the 2θ ranges 14–70° and signals were collected for 20 min. A sample equivalent to 60 mg was placed in sample holder groove and tightly packed.

2.2.9. Near infrared spectroscopy

Near infrared spectroscopy was performed on all the SD formulation using a Foss NIR spectrometer (Rapid Content TM Analyzer, AP-2020, Model 5000, Foss NIR Systems Co., Laurel, MD) equipped with a diffuse reflectance apparatus over the range of 1100–2500 nm. Samples were filled into 2 ml borosilicate glass vials and sextet NIR spectra were collected for each sample by directly scanning the base of vial. Unscramber v9.2 (CAMO Software Inc., Woodbridge, NJ, USA) software was utilized to process and perform chemometric analysis of spectral data.

2.2.10. Tablet compression of solid dispersion

Nine orally disintegrating tablet formulations were manufactured containing SD-3 by direct compression. The composition of tablet formulations (Table 1) was SD-3 (16 mg), Avicel PH 102 (1 mg), diluent (30 mg, mannitol, Flowlac® 100 or galen IQ™-720) and super disintegrant (2.5 mg, glycolys, Ac-Di-Sol or Kollidon® CL-SF). All ingredients were passed through a #40 ASTM sieve and blended for 5 min in a MINIBLEND™ (Globe Pharma Inc., New Brunswick, NJ, USA) at 10 rpm. Magnesium stearate (0.5 mg) was added to the blend which was passed through a #60 ASTM sieve and the final blend was lubricated for 5 min. The tablets were compressed by the Mini Press-1 (Globe Pharma Inc., New Brunswick, NJ, USA) 10-station tabletting machine and 5 mm flat die and punches (Natoli Engineering Company Inc., Saint Charles, MO, USA) with compression data captured by Tablet Press DAQ software. Tablet hardness of all the formulation was maintained within the range of 0.8–1.2 Kp (VK 200 Tablet hardness tester Varian In., Palo Alto, CA). Tablets were assessed for quality control tests such as friability (EF-2 Friabilator, Electrolab, Mumbai, India) and disintegration (in water at 37 °C as per US pharmacopeia, ED-2 Disintegrator testor, Electrolab, Mumbai, India).

2.2.11. Potency and content uniformity test

Twenty tablets were crushed using a mortar and pestle and a powder equivalent to 4 mg of risperidone was transferred into a 50 ml volumetric flask with a volume made up with the mobile phase. The sample was stirred for 10 min on a horizontal shaker at 100 rpm and 25 °C, and then sonicated for 10 min. The samples were filtered through a 0.22 μm Millipore filter and injected into the HPLC system. The experiment was performed in triplicate. For content uniformity, 10 tablets were individually weighed and transferred into a 50 ml volumetric flask and the same procedure was followed as used for the potency test. Calculations were made as per the US Pharmacopeia test for dosage unit uniformity (USP, 2009a,b).

2.2.12. Dissolution test

ODTs were evaluated for dissolution behavior. Dissolution tests used the USP apparatus 2 method in 500 ml of USP phosphate buffer pH 6.0 (0.2 M) at 50 rpm and 37 °C. The dissolution in pH 6.0 medium was chosen to simulate the pH condition of saliva (El-Arini and Clas, 2002), as opposed to 0.1 N HCl as recommended by the FDA (http://www.accessdata.fda.gov/scripts/cder/dissolution/dsp_Sear

Table 1
Orally disintegrating tablet formulation composition and their compression characteristics.

Formulation	Diluents	Super disintegrant	Compression force (lb)	Ejection force (lb)
1	FlowLac® 100	Kollidon® CL-SF	353.10 ± 5.71	11.05 ± 3.53
2	FlowLac® 100	Ac-Di-Sol	421.65 ± 5.28	10.66 ± 5.61
3	galenIQ™-721	Kollidon® CL-SF	262.22 ± 5.82	7.87 ± 6.22
4	galenIQ™-721	Glycolys	311.17 ± 6.28	7.52 ± 9.75
5	Mannitol	Kollidon® CL-SF	456.25 ± 14.13	10.47 ± 11.39
6	FlowLac® 100	Glycolys	391.29 ± 6.71	9.42 ± 6.83
7	Mannitol	Glycolys	589.49 ± 5.22	8.09 ± 7.16
8	Mannitol	Ac-Di-Sol	562.33 ± 7.77	7.65 ± 7.04
9	galenIQ™-721	Ac-Di-Sol	320.49 ± 6.09	6.82 ± 9.91

chResults_Dissolutions.cfm). 1 ml samples were withdrawn at 2, 5, 10 and 15 min, 0.22 μm Millipore filtered and injected into the HPLC for the estimation of risperidone released into the medium. The experiment was performed in triplicate.

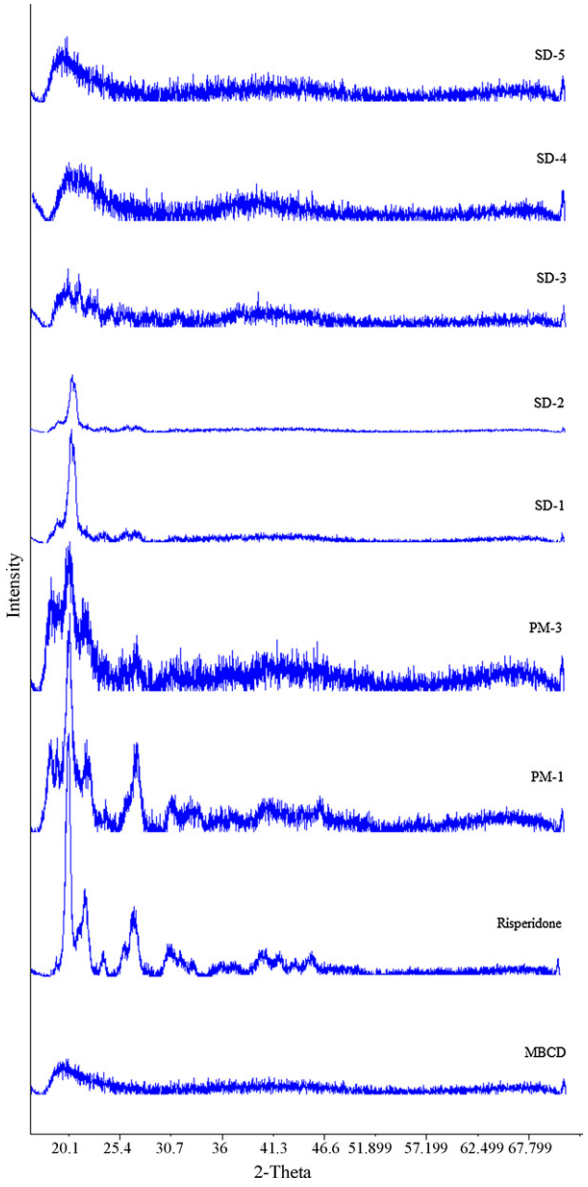

Fig. 4. PXRD spectrum of risperidone, MBCD, their physical mixtures and SD formulations.

2.2.13. Near infrared chemical imaging spectroscopy

The NIR-CI of SD and ODT formulations were collected by SapphireIM NIR Spectral Imaging System (Spectral Dimensions, Inc., Olney, MD). The imaging system consists of a liquid crystal tunable filter (LCTF) coupled with a NIR sensitive focal plane array (FPA) detector. The NIR light reflected (via diffuse reflectance) from the samples to the detector, was passed through a LCTF, and was imaged onto the indium-gallium-arsenide focal plane array with 256 × 320 pixels. Images were recorded from the 1400 to 2450 nm wavelength at 10 nm intervals (105 frames). Dark background was collected with a dark cube (acquired using a stainless steel mirror) and a light background with a high reflectance reference cube (acquired using a Spectralon plate, Labsphere, North Sutton, NH),

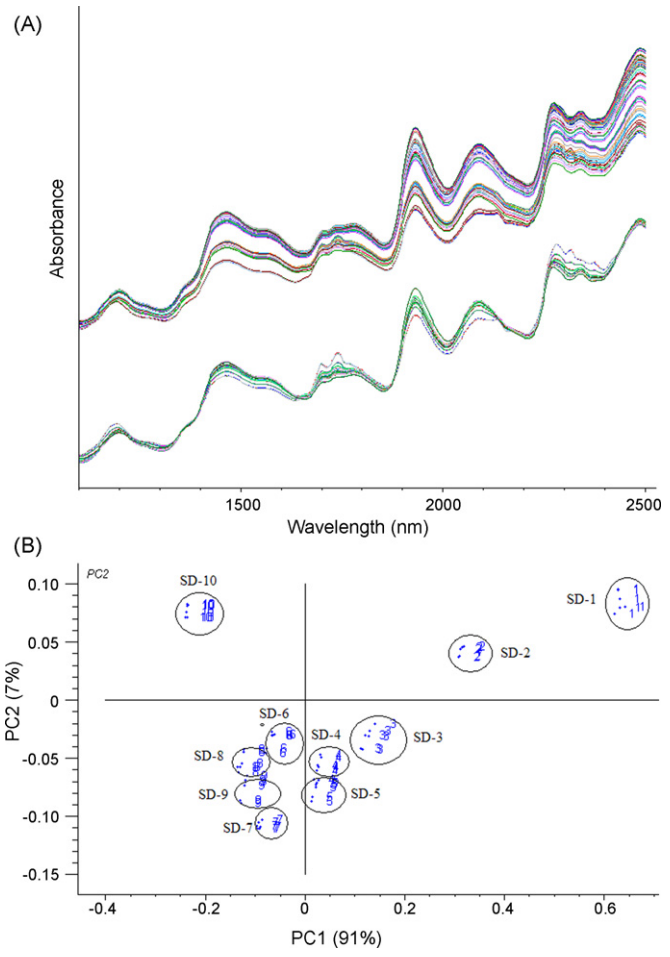

Fig. 5. (A) Original NIR and multiple scattering corrected (MSC) spectra of SD formulations; (B) PC1 and PC2 of MSC-NIR spectra SD formulation computed by principal component analysis.

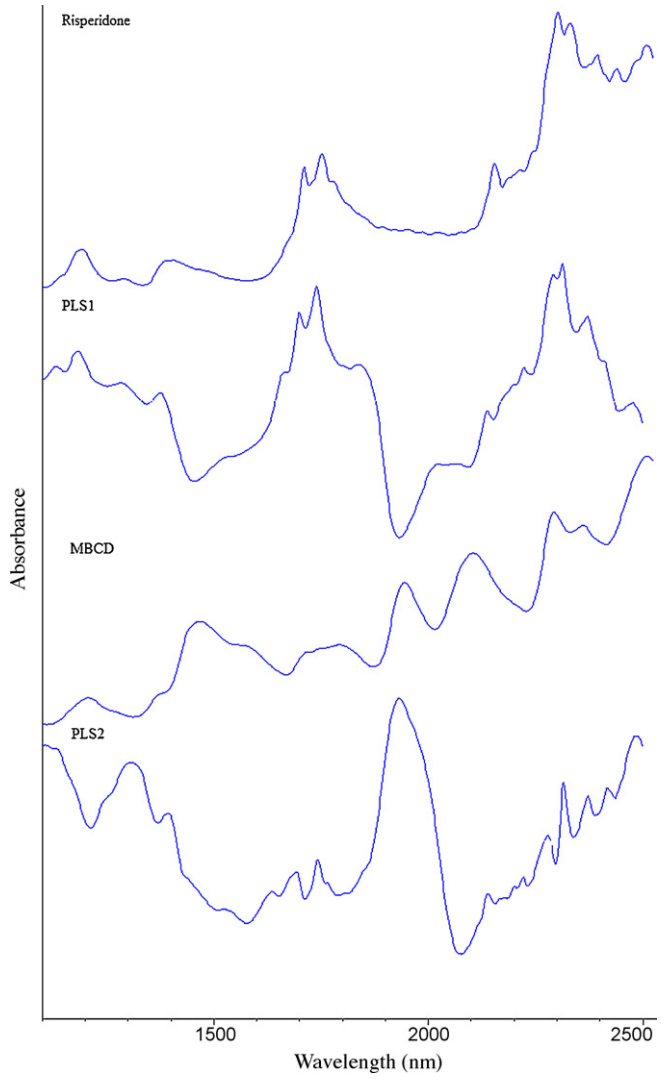

Fig. 6. Loading vectors of the two PLS factors and MSC-NIR spectra of the individual components.

SapphireGo software (Spectral Dimensions, Inc., Olney, MD) automatically subtracted the dark spectrum form the sample cube and then divided by the light background spectrum to produce a corrected reflectance data cube (hyperspectral). Images were analyzed by ISysIM software (Spectral Dimensions, Inc., Olney, MD), each spectrum in the corrected reflectance (R) data cube was converted to absorbance by calculating the logarithm of the inverse of the reflectance ($\log(1/R)$). Each spectrum in the absorbance cube was further differentiated with the Savitzky–Golay second derivative filter with a length of 11 points (100 nm) and a third polynomial order. Pure risperidone and MBCD were used to construct the library. PLS concentration score images were generated using PLS analysis type 2.

3. Results and discussion

3.1. Solid dispersion characterization

3.1.1. Phase solubility study

There was an increase in the solubility of risperidone with MBCD concentration and showed A_L type phase solubility curve (Fig. 1A) which indicated the formation of 1:1 complexation between risperidone and MBCD. Similar results were also reported by other investigators (Danel et al., 2008). The solubility of risperidone in water and 15% (w/w) solution of MBCD at 25 °C was 0.14 ± 0.02 and 13.63 ± 0.08 mg/ml, respectively, which corresponded to a 98.53-fold increased in its solubility.

3.1.2. Physicochemical characteristics of SD formulations

SEM photomicrographs are shown in Fig. 2 with risperidone exhibited as crystalline particles while MBCD were amorphous flakes. The SD formulation showed one type of crystalline particles with a smooth surface and a unique surface morphology different form pure risperidone and MBCD particles. This suggested that the two components were homogeneously distributed in the formulations and a solid solution was formed which could be responsible for the increased dissolution rate of risperidone. FTIR spectrum (Fig. 3A) of risperidone showed absorption bands of C–N stretching between 1000 and 1200 cm^{-1} due to the tertiary amine, 2759–3000 cm^{-1} C–C stretching due to a CH_2 group, 1535 and 3060 cm^{-1} due to C=C stretching of an arene ring and 1643 cm^{-1} due to C=O stretching of an aromatic ketone. The physical mixtures and SD formulations showed the additive spectra encompassing the absorption bands correspond to risperidone and MBCD indicated that no interaction occurred between these two components. The crystallinity and amorphicity of individual components and SD formulations were further tested by DSC and PXRD studies.

The DSC thermogram of the drug (Fig. 3B) showed a sharp endothermic peak at 170 °C corresponding to the melting point of risperidone that further confirmed its crystallinity. MBCD did not show any endo- and/or exothermic peak which indicated its amorphous character. The physical mixtures showed an endothermic peak which corresponded to the risperidone melting point. Similarly, the SD-1 and SD-2 formulations showed characteristic lower intensity endothermic peaks of risperidone than the physical mixtures (PM-1 and PM-3), which indicated that the drug existed in the amorphous and crystalline forms in these SD formulations. SD-3, SD-4 and SD-5 did not show a melting endothermic peak of the drug, that suggested a complete conversion of crystalline drug into its amorphous form or the crystalline portion of the drug was too low in comparison to its amorphous content and possibly, dilution with the MBCD in the SD formulations. A similar trend was seen in the X-ray diffractogram studies (Fig. 4). The diffractogram of risperidone exhibited its crystalline nature as indicated by peaks at 2θ value of 19.7°, 20.6°, 22.43°, 24.58°, 27.33°, 31.79° and 43.79° while MBCD did not show any peak in its diffractogram which confirmed its amorphicity. The physical (PM-1 and PM-3) mixture showed the characteristic peaks of risperidone while SD-1 and SD-2 formulation showed a peak at 20.6° that disappeared in SD-3, SD-4 and SD-5. Consequently, PXRD studies confirmed the finding of the DSC studies.

3.1.3. Dissolution rate

Dissolution profiles of the SD formulations are shown in Fig. 1B. All the SD formulations dissolved more than 90% risperidone in 15 min. There were significant differences in the dissolution profiles of raw risperidone, physical mixture and SD formulations. The formulations can be arranged in an increasing order of risperidone released in 15 min as follows: raw risperidone < PM-5 < SD-1 < SD-2 < SD-3 < SD-4 < SD-5. There was a progressive increase in the percentage of risperidone dissolved in 2 min from 72.17 ± 1.30 to 95.96 ± 8.95% in SD-1 and SD-3, respectively. PM-5 has same weight ratio composition of SD-5 but dissolved 38.16 ± 6.95% in 15 min while complete dissolution was observed from SD-5 in 2 min. The increase in the dissolution of risperidone with MBCD concentration could be explained by the principal of hydrophilicity, inclusion complex formation and the amorphous form generation of risperidone. The high solubility of MBCD in water resulted in better wettability of drug particles and local enhancement of

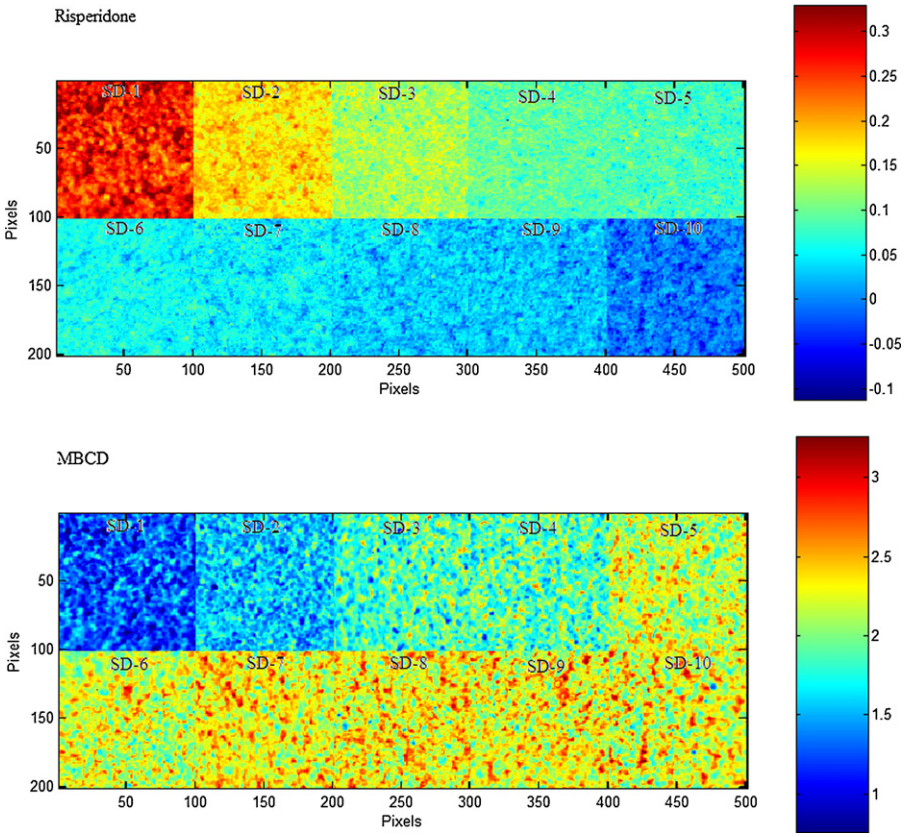

Fig. 7. PLS images showing the distribution of risperidone and MBCD in the SLN formulation.

its solubility at the diffusion layer surrounding the drug particles. Subsequently, the interaction between the hydrophobic drug molecule and hydrophobic cavity of MBCD resulted in the formation of an inclusion complex (Wang et al., 2009). The percentage drug dissolved from SD formulations was higher compared to its corresponding physical mixture. This could be explained by the generation of the amorphous form of risperidone in the SD formulations during the manufacturing step and in general the amorphous form of a substance has a higher dissolution rate than its crystalline form (Rahman et al., 2010a).

3.2. Orally disintegrating tablet characterization

3.2.1. Disintegration time

Tablet characteristics were shown in Table 2. ODT formulations passed in potency and content uniformity specification for risperidone tablets as per the US Pharmacopeia (USP, 2009a,b). The FDA recommends a disintegration time of 30 s or less for ODTs based on the USP disintegration test (FDA guidance, 2008). Superdisintegrants are commonly used to reduce the disintegration time and to speed drug release and potentially increase the absorption process of a drug. They are used in low concentration usually 1–10% of tablet weight. The mechanism by which they reduce the disintegration time is swelling, wicking and volume expansion (Quadir and Kolter, 2006). DT (disintegration time) of the ODT formulations varied from 22.83 ± 3.66 (formulation-8) to 122.80 ± 14.50 s (formulation-4) (Table 2). The formulations could be arranged in a decreasing order of their DT as formulation-4 > formulation-9 > formulation-6 > formulation-2 > formulation-3 > formulation-7 > formulation-1 > formulation-5 > formulation-8. Statistical evaluation of DT of ODTs revealed that formulations 5 and 8 were statistically significant ($p < 0.05$) from the other formulations. These two formulations have the smallest DT contained mannitol as a diluent. Formulations 4 and 9 showed the longest DT based on galenIQ^{TM}-721 (maltose) as a diluent. These results were in agreement with the findings of other investigator (Mizumoto et al., 2005). This phenomenon could be explained by surface free energy and compressibility phenomenon. The lactose (FlowLac® 100), and mannitol and maltose (galenIQ^{TM}-721) have low and high surface free energy. Furthermore, maltose, and lactose and

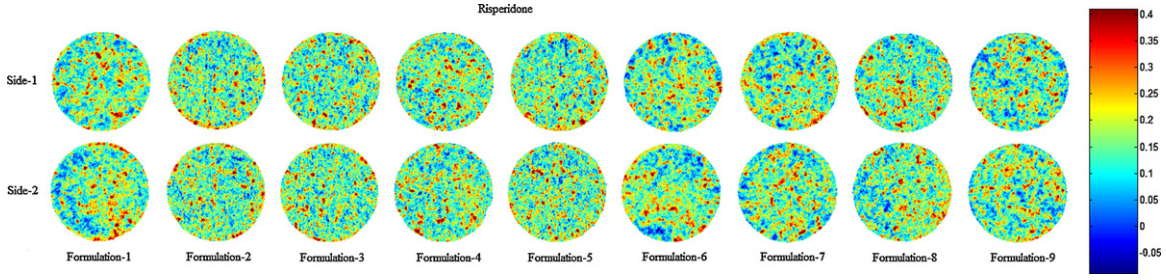

Fig. 8. PLS images showing the distribution of risperidone in the ODT formulation.

Table 2
Results of orally disintegrating tablet formulations. Value indicated as mean ± S.D.

Formulation	Content uniformity (range, %)	Friability (%)	Potency (%)	Disintegration time (s)	T_{50} (s)	T_{90} (s)
1	98.12–101.45	1.58	98.56 ± 1.23	37.50 ± 1.97	3.78 ± 0.29	9.36 ± 0.01
2	97.23–99.01	2.22	98.45 ± 2.01	75.50 ± 5.79	4.04 ± 0.38	10.84 ± 2.41
3	97.34–98.95	2.27	102.34 ± 3.87	69.67 ± 3.72	3.45 ± 0.17	8.73 ± 0.09
4	95.45–99.19	1.86	97.93 ± 3.06	122.80 ± 14.50	4.63 ± 0.37	15.69 ± 1.39
5	97.07–102.04	2.31	97.67 ± 2.76	24.67 ± 6.45	1.69 ± 0.61	7.95 ± 0.93
6	98.56–103.11	3.37	99.05 ± 0.81	84.00 ± 6.45	4.12 ± 0.43	11.70 ± 0.82
7	97.17–102.06	3.30	102.71 ± 1.61	42.60 ± 5.13	3.05 ± 0.20	10.10 ± 1.41
8	94.94–99.77	2.87	98.87 ± 1.05	22.83 ± 3.66	2.43 ± 0.22	8.94 ± 0.77
9	97.67–101.35	1.68	98.66 ± 2.98	104.40 ± 8.68	3.80 ± 0.14	9.28 ± 0.12

mannitol have eight and six free hydroxyl group, respectively. All these factors contributed to stronger cohesion force between the particles of galenIQ™-721 (maltose) than mannitol, which contributed to lengthening of DT in galenIQ™-721 based ODT formulations (Mizumoto et al., 2005). Similarly, Kollidon® CL-SF decreased the disintegration time whereas sodium starch glycolate prolonged the value of DT. These observation could be explained by the fact of Kollidon ability to reach 90% maximum swelling pressure in a short period (32.9 s) compared to sodium starch glycolate and Ac-D-Sol (75 and 88.1 s, respectively) (Quadir and Kolter, 2006).

3.2.2. T_{50} and T_{90}

T_{50} and T_{90} are the time required to release 50 and 90% of risperidone from ODT formulations, respectively. The value of T_{50} and T_{90} varied from 1.69 ± 0.22 (formulation 5) to 4.63 ± 0.37 s (formulation 4), and 7.95 ± 0.93 (formulation 5) to 15.69 ± 1.39 s (formulation 4), respectively (Table 2). T_{50} and T_{90} of formulations 5 and 8 were statistically significant ($p < 0.05$) when compared with the other ODT formulations. Mannitol and Kollidon® CL-SF decreased while galenIQ™-721 and sodium starch glycolate increased T_{50} and T_{90} value. This was due to the effect of these variables on their DT values and a good correlation was obtained between T_{50} and DT, and T_{90} and DT as revealed by '*R*' values of 0.83 and 0.73, respectively.

3.3. Chemometrics

3.3.1. Near infrared spectroscopy

The major obstacle in successful estimation of components of dosage is the variation in NIR collected data due to multiplicative scattering arising due to different packing density of a sample (Heigl et al., 2009) and baseline shift (Smith and Baker, 1981). This variation can be minimized or removed by post-collection mathematical treatment of data such as first derivative, second derivative, second derivative logarithm (SDL) (Tahboub and Pardue, 1985), standard normal variant (SNV) (Barnes et al., 1989) and multiple scattering correction (MSC) (Geladi et al., 1985). SDL can remove the parallel baseline shift but can add noise to data which make its interpretation difficult. SNV and MSC are the most common methods for removal of multiple scattering and can also correct the background slope in the data.

Raw NIR data of SD formulations are shown in Fig. 5A. Data were pretreated with first derivative, second derivative and SNV to remove baseline shifting and multiple scattering. None of the methods were effective in removing these effects except MSC (Fig. 5A). The SD formulations data were divided into calibration and validation set based on the drug loading in the SD formulations for constructing the models. SD-2, SD-3, SD-6, SD-8 and SD-10 were selected for calibration samples and contained 33.33, 25, 14.29, 11.11 and 9.09% of risperidone, respectively. Similarly, formulation SD-1, SD-4, SD-5, SD-7 and SD-9 were chosen for validation samples and have 50, 20, 16.67, 12.50 and 10% of drug, respectively. The MSC data was subjected to principal component analysis (two components) to analyze the data distribution. The scores of PC1 and PC2 of calibration and prediction data represented 91 and 7% variations in the data set, respectively (Fig. 5B). PCA allowed successful scattering of SD formulation and their approximate PC1 scores were 0.65, 0.32, 0.15, 0.02, −0.07, −0.10, −0.14, −0.15 and −0.25. The SD formulations arranged according to increased MBCD or decreased risperidone loading with PC1 scores: SD-1 > SD-2 > SD-3 > SD-4 > SD-5 > SD-6 > SD-7 > SD-8 > SD-9 > SD-10. This trend suggested that PC1 either related to MBCD or risperidone loading in the SD formulations.

The NIR spectroscopy reflects change in its spectrum due to alteration in the chemical and physical property in the sample. This change can be correlated with the property of interest of sample and can be use for qualitative and quantitative analysis. The most commonly used statistical tool to construct the chemometric model based on spectroscopy data is the partial least square (PLS) method of multiple regressions because it is less restrictive and flexible nature over other method of multiple regressions. Chemometric models constructed by the PLS method can be used to estimate components of binary or higher order mixtures (Baratieri et al., 2006). PLS was applied using two PLS factors. PLS1 and PLS2 factors represented 91 and 7% variation of MSC-NIR data of the SD formulation, respectively. Statistics of PLS analysis of calibration and prediction data set was given in Table 3 for risperidone and MBCD. Good correlation was shown between the predicted and measured values of the calibration and validation set for the risperidone and

Table 3
Results of PLS regression of MSC-NIR data for calibration and prediction of risperidone and MBCD from SD formulations.

Parameters	MSC-NIR			
	Risperidone		MBCD	
	Calibration	Prediction	Calibration	Prediction
Number of sample	30	30	30	30
Correlation	0.9965	0.9973	0.9965	0.9973
Offset	0.1301	1.1090	0.5708	2.7338
Slope	0.9929	0.9616	0.9929	0.9616
Root mean square of error	0.7702	1.1909	0.7702	1.1909
Standard error	0.7833	1.1797	0.7833	1.1797

Table 4
Results of histogram distributions from PLS score images of SD formulations.

Formulation	Risperidone			MBCD		
	Number of pixel	Mean ± S.D.	Skewness	Number of pixel	Mean ± S.D.	Skewness
SD-1	9906	0.4185 ± 0.0379	0.2351	9980	1.3 ± 0.2047	0.1852
SD-2	9938	0.2494 ± 0.0299	0.0628	9965	1.5 ± 0.1892	0.1727
SD-3	9941	0.1603 ± 0.0276	0.0177	9939	1.9 ± 0.223	0.1235
SD-4	9960	0.1052 ± 0.0274	−0.0389	9965	1.9 ± 0.2322	0.1862
SD-5	9938	0.0945 ± 0.0250	−0.0705	9977	2.2 ± 0.2222	0.1184
SD-6	9967	0.0700 ± 0.0259	−0.0142	9965	2.2 ± 0.2205	0.1933
SD-7	9927	0.0617 ± 0.0272	−0.1314	9963	2.3 ± 0.2316	0.2067
SD-8	9919	0.0273 ± 0.0280	−0.0868	9955	2.3 ± 0.2519	0.0879
SD-9	9955	0.0345 ± 0.0250	−0.0207	9943	2.3 ± 0.2473	0.2439
SD-10	9956	0.0092 ± 0.0242	−0.0587	9941	2.3 ± 0.2659	0.2925

MBCD as indicated by the correlation coefficient values of >0.9965 in all cases (Table 3). Furthermore, the model showed good prediction ability as suggested by the smaller values of root mean square error of calibration and prediction (RMSEP, RMSEP) and standard errors of calibration and prediction (SEC, SEP) suggested model equivalency in simultaneously estimation of the components of the SD formulations.

Mean bias and mean accuracy were determined using following equation to assess the accuracy of the calibration curve based on the validation data set (Suda et al., 2008).

$$B_m = \frac{\sum_{i=1}^{n}(X_c - X_t)/X_t}{n} \times 100$$

$$A_m = \frac{\sum_{i=1}^{n}|X_c - X_t|/X_t}{n} \times 100$$

where B_m is the percentage mean bias, A_m is the percentage mean accuracy, X_c is the predicted drug/polymer loading value, X_t is the actual drug/polymer loading and n is the number of experiments. The mean accuracy and mean bias for risperidone and MBCD predictions from MSC-NIR data were 6.63 and 1.28%, and 3.55 and −0.19% suggesting that the model is more accurate in predicting MBCD than risperidone.

Chemometric models based on PLS can split the raw spectral data into individual PLS factors and identify significant contributions of these factors to the physical and chemical property of interest. The loading vectors of the PLS factors were compared with the spectra of individual components (Fig. 6). PLS1 showed the positive peaks at 2376, 2314, 2294, 2222, 1738, 1698, 1378, 1182 and 1136 nm and negative peaks at 2474, 2136 and 2010 nm which can be attributed to risperidone. Similarly, PLS2 showed positive peaks and negative peaks at 2416, 2370, 2314, 2278, 1930, 1394 and 1318 nm, and 2222, 2138, 1742, 1692 and 1626 nm, respectively which could be due to MBCD.

3.3.2. Near infrared chemical imaging

NIR-CI can provide the spatial distribution of a chemical entity in addition to providing information on spectral information of a chemical entity in a compound. This non-destructive technique finds its application in the identification of counterfeit drug products (Puchert et al., 2010), the assessment of homogeneity of pharmaceutical blends (Gendrin et al., 2008), distribution and concentration of active substance in dosage forms (Rahman et al., 2010a,b; Zidan et al., 2009) and the identification, and discrimination of polymorphic forms (LaPlant, 2004).

NIR-CI PLS images of the SD formulations were shown in the Fig. 7 and concatenated according to risperidone and MBCD from the prebuilt binary component library containing risperidone and MBCD. The images showed homogenous distribution of risperidone and MBCD which was further supported by their histogram (not shown) and lower value of skew (Fig. 7, Table 4). The PLS images represented either risperidone or MBCD could be arranged according to their mean concentration and rank order of SD formulation according to mean concentration of risperidone were SD-1 > SD-2 > SD-3 > SD-4 > SD-5 > SD-6 > SD-7 > SD-8 > SD-9 > SD-10 and order would be reversed if arranged according to MBCD mean concentration which was in agreement with actual risperidone or MBCD loading in the SD formulations. The components of SD formulations could be quantitated by plotting the quantile–quantile plot between the actual risperidone or MBCD loading and the mean concentration of risperidone or MBCD from their PLS concentration images (Table 4) with a R^2 of 0.9943 for risperidone and no correlation for MBCD. Similarly, the PLS concentration images of ODT tablet formulations are shown in Fig. 8 according to risperidone concentration. These images indicated the homogeneity of risperidone distribution in the tablet formulations, with no difference in side 1 and side 2 of the same tablet.

4. Conclusions

The solid dispersion of risperidone with methyl-β-cyclodextrin greatly enhanced its dissolution rate. The mannitol and Kollidon®CL-SF showed a negative impact whereas galenIQ™-721 and sodium starch glycolate have positive impact on disintegration time, T_{50} and T_{90} of ODTs of risperidone containing SD. The SD of risperidone was homogenously distributed as indicated by their NIR-CI images. PLS-MSC chemometric model based on NIR data of solid dispersions indicated good correlation for the calibration and validation. The model was equivalent in simultaneously estimating risperidone and MBCD from SD formulations as indicated by a lower root mean square and standard error of the calibration and prediction. Thus, NIR chemical imaging provided another non-destructive method for the estimation of components of solid dispersions.

Acknowledgement

The authors would like to thank the Oak Ridge Institute for Science and Education (ORISE) for supporting post doctoral research program.

References

Ahmed, I., Aboul-Einien, M., 2007. In vitro and in vivo evaluation of a fast disintegrating lyophlised dry emulsion tablet containing griseofulvin. Eur. J. Pharm. Sci. 32, 58–68.
Alcala, M., Blanco, M., Bautista, M., González, J.M., 2009. On-line monitoring of a granulation process by NIR spectroscopy. J. Pharm. Sci. 99, 336–345.
Amidon, G.L., Lennernas, H., Shah, V.P., Crison, J.R., 1995. A theoretical basis for biopharmaceutic drug classification: the correlation of in vitro drug product dissolution and in vivo bioavailability. Pharm. Res. 12, 413–420.
Babu, R.J., Dayal, P., Singh, M., 2008. Effect of cyclodextrins on the complexation and nasal permeation of melatonin. Drug Deliv. 15, 381–388.

Baratieri, S.C., Barbosa, J.M., Freitas, M.P., Martins, J.A., 2006. Multivariate analysis of nystatin and metronidazole in a semi-solid matrix by means of diffuse reflectance NIR spectroscopy and PLS regression. J. Pharm. Biomed. Anal. 40, 51–55.

Barnes, R.J., Dhanoa, M.S., Lister, S.J., 1989. Standard normal variate transformation and de-trending of near-infrared diffuse reflectance spectra. Appl. Spectrosc. 43, 772–777.

Biradar, S.S., Bhagavaati, S.T., Kuppasad, I.J., 2006. Fast dissolving drug delivery systems: a brief overview. Int. J. Pharmacol. 4.

Brewster, M.E., Loftsson, T., 2007. Cyclodextrins as pharmaceutical solubilizers. Adv. Drug Deliv. Rev. 59, 645–666.

Chen, R., Takahashi, H., Okamoto, H., Danjo, K., 2006. Particle design of three-component system for sustained release using a 4-fluid nozzle spray-drying technique. Chem. Pharm. Bull. (Tokyo) 54, 1486–1490.

Cirri, M., Maestrelli, F., Mennini, N., Mura, P., 2009. Influence of the preparation method on the physical-chemical properties of ketoprofen-cyclodextrin-phosphatidylcholine ternary systems. J. Pharm. Biomed. Anal. 50, 690–694.

Corveleyn, S., Remon, J., 1998. Formulation of a lyophilised dry emulsion tablet for the delivery of poorly soluble drugs. Int. J. Pham. 166, 65–74.

Danel, C., Azaroual, N., Brunel, A., Lannoy, D., Vermeersch, G., Odou, P., Vaccher, C., 2008. Study of the complexation of risperidone and 9-hydroxyrisperidone with cyclodextrin hosts using affinity capillary electrophoresis and ^{1}H NMR spectroscopy. J. Chromatogr. A 1215, 185–193.

Dhopeshwarker, V., Kowal, R., Mattes, R.A., Randolph, W., Schroeder, R., 2005. Monitoring granulation drying using near-infrared spectroscopy. Pharm. Tech. Eur. 17, 41–45.

El-Arini, S.K., Clas, S.D, 2002. Evaluation of disintegration testing of different fast dissolving tablets using the texture analyzer. Pharm. Dev. Tech. 7, 361–371.

Food and Drug Administration – Guidance for Industry – Orally Disintegrating Tablet. Silver Spring, Maryland, USA, 2008.

Geladi, P., MacDougall, D., Martens, H., 1985. Linearization and scatter-correction for near-infrared reflectance spectra of meat. Appl. Spectrosc. 39, 491–500.

Gendrin, C., Roggo, Y., Spiegel, C., Collet, C., 2008. Monitoring galenical process development by near infrared chemical imaging: one case study. Eur. J. Pharm. Biopharm. 68, 828–837.

Ghorab, M.M., Abdel-Salam, H.M., El-Sayad, M.A., Mekhel, M.M., 2004. Tablet formulation containing meloxicam and beta-cyclodextrin: mechanical characterization and bioavailability evaluation. AAPS PharmSciTech 5, e59.

Heigl, N., Petter, C.H., Lieb, M., Bonn, G.K., Huck, C.W., 2009. Near-infrared reflection spectroscopy and partial least squares regression for determining the total carbon coverage of silica packings for liquid chromatography. Vib. Spectrosc. 49, 155–161.

http://www.accessdata.fda.gov/scripts/cder/dissolution/dsp_SearchResults_Dissolutions.cfm (accessed on April 01, 2010).

International Conference of Harmonization-Validation of Analytical Procedures Q2(R1), 2005.

Kanagale, P., Patel, V., Venkatesan, N., Jain, M., Patel, P., Misra, A., 2008. Pharmaceutical development of solid dispersion based osmotic drug delivery system for nifedipine. Curr. Drug Deliv. 5, 306–311.

Khan, M.A., Karnachi, A.A., Agarwal, V., Vaithiyalingam, S.V., Nazzal, S., Reddy, I.K., 2000. Stability characterization of controlled release coprecipitates and solid dispersions. J. Control. Release 63, 1–6.

Klein, S., Wempe, M.F., Zoeller, T., Buchanan, N.L., Lambert, J.L., Ramsey, M.G., Edgar, K.J., Buchanan, C.M., 2009. Improving glyburide solubility and dissolution by complexation with hydroxybutenyl-beta-cyclodextrin. J. Pharm. Pharmacol. 61, 23–30.

LaPlant, F., 2004. Factors affecting NIR chemical images of solid dosage forms. Am. Pharm. Rev. 7, 16–24.

Li, W., Bagno, l.L., Berman, M., Chiarella, R.A., Gerber, M., 2009. Applications of NIR in early stage formulation development. Part II. Content uniformity evaluation of low dose tablets by principal component analysis. Int. J. Pharm. 380, 49–54.

Liu, C., Zhu, S.J., Zhou, Y., Wei, Y.P., Pei, Y.Y., 2006. Enhancement of dissolution of cyclosporine A using solid dispersions with polyoxyethylene (40) stearate. Pharmazie 61, 681–684.

Mannila, J., Järvinen, T., Järvinen, K., Jarho, P., 2007. Precipitation complexation method produces cannabidiol/beta-cyclodextrin inclusion complex suitable for sublingual administration of cannabidiol. J Pharm Sci 96 (2), 312–321.

Mathot, F., van Beijsterveldt, L., Preat, V., Brewster, M., Arien, A., 2006. Intestinal uptake and biodistribution of novel polymeric micelles after oral administration. J. Control. Release 111, 47–55.

Mizumoto, T., Masuda, Y., Yamamoto, T., Yonemochi, E., Terada, K., 2005. Formulation design of a novel fast-disintegrating tablet. Int. J. Pharm. 306, 83–90.

Patel, A.R., Vavia1, P.R., 2008. Preparation and evaluation of taste masked famotidine formulation using drug/β-cyclodextrin/polymer ternary complexation approach. AAPS PharmSciTech 9, 544–550.

Puchert, T., Lochmann, D., Menezes, J.C., Reich, G., 2010. Near-infrared chemical imaging (NIR-CI) for counterfeit drug identification—a four-stage concept with a novel approach of data processing (Linear Image Signature). J. Pharm. Biomed. Anal. 51, 138–145.

Quadir, A., Kolter, K., 2006. A comparative study of current superdisintegrants. Pharm. Technol. (October).

Rahman, Z., Kohli, K., Khar, R.K., Ali, M., Charoo, N.A., Shamsher, N.A., 2006. Characterization of 5-fluorouracil microspheres for colonic delivery. AAPS PharmSciTech 7, E1–E9.

Rahman, Z., Zidan, A.S., Habib, M.J., Khan, M.A., 2010a. Formulation and evaluation of a protein loaded solid dispersions by non-destructive methods. AAPS J. 12, 158–170.

Rahman, Z., Zidan, A.S., Habib, M.J., Khan, M.A., 2010b. Non-destructive methods of characterization of risperidone solid lipid nanoparticles. Eur. J. Pharm. Biopharm. (May 12 Epub).

Rahamathulla, M., Hv, G., Rathod, N., 2008. Solubility and dissolution improvement of rofecoxib using solid dispersion technique. Pak. J. Pharm. Sci. 21, 350–355.

Rantanen, J., Wikström, H., Turner, R., Taylor, L.S., 2005. Use of in-line near-infrared spectroscopy in combination with chemometrics for improved understanding of pharmaceutical processes. Anal. Chem. 77, 556–563.

Ryan, J.A., Compton, S.V., Brooks, M.A., Compton, D.A., 1991. Rapid verification of identity and content of drug formulations using mid-infrared spectroscopy. J. Pharm. Biomed. Anal. 9, 303–310.

Sekulic, S.S., Ward, H.W., Brannegan, D.R., Stanley, E.D., Evans, C.L., Sciavolino, S.T., Hailey, P.A., Aldridge, P.K., 1996. On-line monitoring of powder blend homogeneity by near-infrared spectroscopy. Anal. Chem. 68, 509–513.

Smith, R.C., Baker, K.S., 1981. Optical properties of clearest natural waters (200–800 nm). Appl. Opt. 20, 177–184.

Suda, M., Takayama, K., Otsuka, M., 2008. An accurate quantitative analysis of polymorphic content by chemometric X-ray powder diffraction. Anal. Sci. 24, 451–457.

Sulub, Y., Wabuyele, B., Gargiulo, P., Pazdan, J., Cheney, J., Berry, J., Gupta, A., Shah, R., Wu, H., Khan, M.A., 2009. Real-time on-line blend uniformity monitoring using near-infrared reflectance spectrometry: a noninvasive off-line calibration approach. J. Pharm. Biomed. Anal. 49, 48–54.

Suthar, A.P., Dubey, S.A., Patel, S.R., Shah, A.M., 2009. Determination of risperidone and forced degradation behavior by HPLC in tablet dosage form. Int. J. PharmTech. Res. 1, 568–574.

Tahboub, Y.R., Pardue, H.L., 1985. Evaluation of multiwavelength first- and second-derivative spectra for the quantitation of mixtures of polynuclear aromatic hydrocarbons. Anal. Chem. 57, 38–41.

Tewes, F., Brillault, J., Couet, W., Olivier, J.C., 2008. Formulation of rifampicin-cyclodextrin complexes for lung nebulization. J. Control. Release 129, 93–99.

USP-32-NF-27 Risperidone Tablet 3519, 2009. Rockville, Maryland, United States.

USP-32-NF-27 Uniformity of Dosage Unit (905) 382, 2009. Rockville, Maryland, United States.

Wang, S., Ding, Y., Yao, Y., 2009. Inclusion complexes of fluorofenidone with beta-cyclodextrin and hydroxypropyl-beta-cyclodextrin. Drug Dev. Ind. Pharm. 31, 1–6.

Zidan, A.S., Rahman, Z., Habib, M.J., Khan, M.A., 2010. Spectral and spatial characterization of protein loaded PLGA nanoparticles. J. Pharm. Sci. 99, 1180–1192.